Convective Cellular Flow in a Horizontally Long Layer of Fluid

Koga, Seiko
Department of Earth System Science and Technology, Interdisciplinary Graduate School of Engineering Sciences, Kyushu University

Honji, Hiroyuki
Department of Earth System Science and Technology, Interdisciplinary Graduate School of Engineering Sciences, Kyushu University

Matsunaga, Nobuhiro
Department of Earth System Science and Technology, Interdisciplinary Graduate School of Engineering Sciences, Kyushu University

Sugihara, Yuji
Department of Earth System Science and Technology, Interdisciplinary Graduate School of Engineering Sciences, Kyushu University

https://doi.org/10.15017/17310

出版情報：九州大学大学院総合理工学報告. 15 (2), pp.217-225, 1993-09-01. 九州大学大学院総合理工学研究科

九州大学大学院総合理工学研究科報告
第15巻 第2号 217-225頁 平成5年9月

Engineering Sciences Reports, Kyushu University
(KYUSHU DAIGAKU SOGORIKOGAKU KENKYUKA HOKOKU)
Vol. 15, No. 1, pp. 217 - 225, SEPT. 1993

Convective Cellular Flow in a Horizontally Long Layer of Fluid

Seiko KOGA*, Hiroyuki HONJI**, Nobuhiro MATSUNAGA**,
and Yuji SUGIHARA**

(Received May 28, 1993)

The formation of heat-driven two-dimensional convective cellular flow in a horizontally long layer of fluid has been investigated experimentally at $1.40\times10^4 \leqq Ra \leqq 1.2\times10^6$ and $4.80\times10^3 \leqq Pr \leqq 6.00\times10^3$, Ra and Pr being respectively the Rayleigh and Prandtl numbers. The numerically obtained value for the ratio of the horizontal mean wavelength of cell paires to fluid depth at large Ra agrees approximately with its experimental value of 1.7, although the range of Pr is much smaller than the above mentioned experimental range.

1. Introduction

Heat-driven convective flows form commonly in such geofluids as atmosphere, oceans, and mantles. Many theoretical and experimental studies have been concerned with diverse phenomena of thermal convection. Its physical and geophysical aspects are summarized, for example, in Normand & Pomeau[1] and Turner[2], respectively. In particular, Bolton and Busse[3] studied the structure of stable two-dimensional (2D) rolls at Rayleigh numbers (Ra) below 2×10^4. Schnaubelt and Busse[4] studied the range of Ra for the appearance of stable rolls. These studies are concerned with stationary thermal convection. Kanda and Hino[5] directed their attention to the time evolution of convection, and studied the effect of phase change on the merging of convective cells, which may be relevant to the development of cumulus clouds.

The present study is concerned with the structure and time-evolution of cellular flow in a horizontally long 2D layer of fluid in a tank. The paper is organized as follows: in section 2 are described the experimental methods and results and in section 3 the numerical methods and discussion. Section 4 is devoted to the conclusions.

2. Experiments

2.1 Experimental methods

The experiments were carried out using a fluid tank illustrated in **Fig. 1**. The tank is made of transparent acrylic resin plates with the thickness of 10 mm, and its dimensions are 600 mm in horizontal length, 400 mm in depth, and 20 mm in width. This tank was filled with glycerine as a working fluid up to the depth H. In **Fig. 1** is also indicated L, which is the horizontal wavelength of a stationary cellular flow, i.e. the horizontal scale of a cell pair. In the above setup, the glycerine layer was quite long in a horizontal direction and

*Graduate Student, Department of Earth System Science and Technology
**Department of Earth System Science and Technology

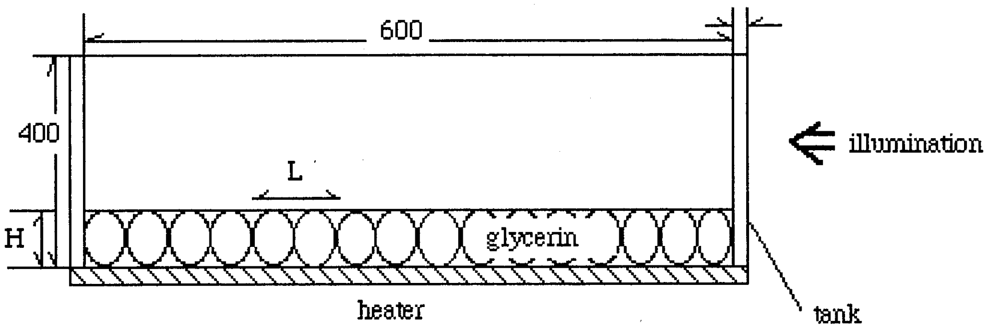

Fig. 1 Experimental tank (Dimensions in mm)

thin in the other horizontal direction to provide a 2D flow domain.

The fluid layer was heated uniformly from below using a 12W straight rod heater, which was controlled with a slidac. The properties of glycerine at 20℃ are: the volume expansion coefficient $\beta = 4.700 \times 10^{-2} K^{-1}$, kinematic viscosity $\nu = 1.183 \times 10^{-3} m^2/s$, and thermal diffusion coefficient $\kappa = 9.280 \times 10^{-6} m^2/s$. Convective flows established in the tank were visualized with suspended aluminum dusts illuminated from side using a 1kW slide projector.

The time-wise variations of glycerine and room temperatures are shown in **Fig. 2.** The room temperature was adjusted to be 24.0℃ by using an air conditioner. In the figure the temperature difference between lower (near-bottom) and upper (near-surface) glycerine layers is denoted as Δ T, which is nearly constant at 8.00℃ at later times. Temperatures in the grycerine were measured with a thermocouple system.

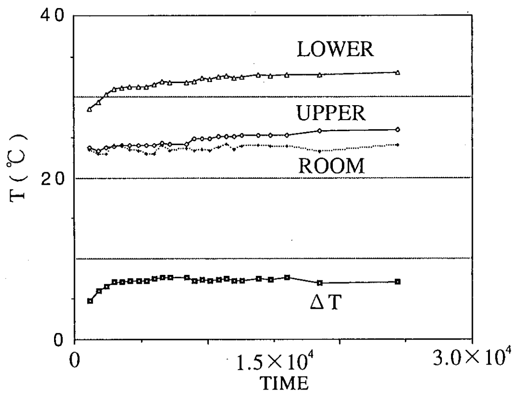

Fig. 2 Time-wise variation of fluid and room temperatures

The two main dimensionless parameters relevant to the present study are Rayleigh and Prandl numbers, which are defined as

$$Pr = \frac{\nu}{\kappa} \tag{1}$$

and

$$Ra = \frac{g \beta \Delta T H^3}{\kappa \nu} \tag{2}$$

Table 1. Parameter values relevant to the experiments

	H (m)	ν (m^2/s)	Ra	Pr
1	0.025	4.45×10^{-4}	1.40×10^{4}	4.80×10^{3}
2	0.03	4.90×10^{-4}	2.20×10^{4}	5.30×10^{3}
3	0.04	4.90×10^{-4}	5.20×10^{4}	5.30×10^{3}
4	0.06	5.34×10^{-4}	1.60×10^{5}	5.80×10^{3}
5	0.12	5.60×10^{-4}	1.20×10^{6}	6.00×10^{3}

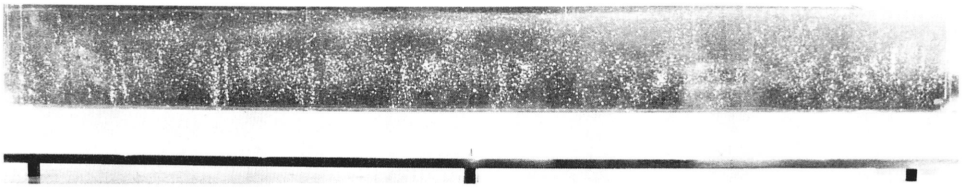

(a) $\hat{t}=250$

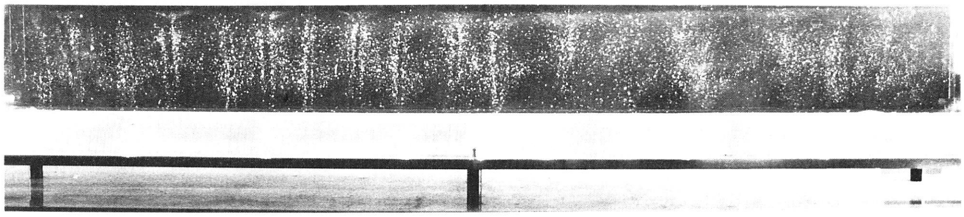

(b) $\hat{t}=270$

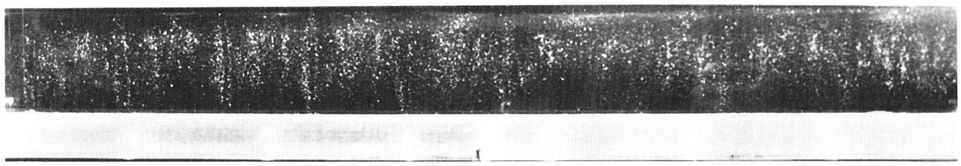

(c) $\hat{t}=360$

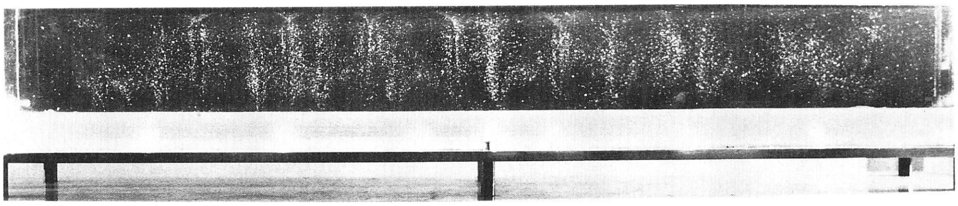

(d) $\hat{t}=530$

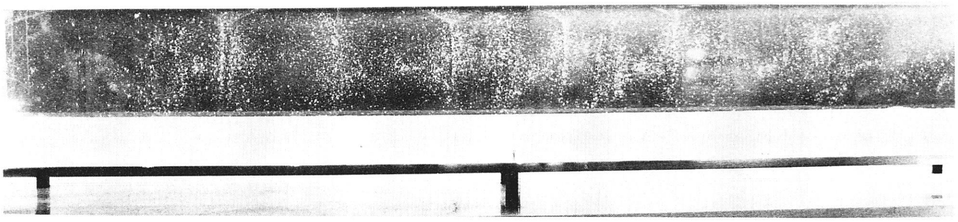

(e) $\hat{t}=930$

Fig. 3 Time-wise development of convective cells at $Ra=1.60\times10^{5}$, $Pr=5.80\times10^{3}$, and $H=0.06$ m where g is the acceleration due to gravity. The parameter values are tabulated in **Table 1.**

The other relevant dimensionless numbers are the aspect ratio for a cell pair L/H and the dimensionless time $\hat{t}$, which is defined as

$$\hat{t}=t\cdot\frac{\nu}{H^2} \quad , \tag{3}$$

where t is the time measured from the onset of heating.

2.2 Experimental Results

An example of time-wise development of a cellular flow is shown in **Fig. 3**, where $\hat{t}$ ranges from 250 to 930. It will be seen from the photographs that the forms and positions of the cells change with time. The merging of neighbouring cells may be responsible for this change, which gives rise to an increase of L with $\hat{t}$.

The phenomenon of a cell-pair merging is also shown in **Fig. 4**, where t ranges from 720 to 1010. The values of H, Ra, and Pr are the same as those for **Fig. 3**. There are initially the three cell pairs consisting of six cells between the two arrows indicated below the photograph of **Fig. 4(a)**. As time goes on, the cell boundaries lose their sharpness because of occurrence of merging of the cells as seen from **Fig. 4(b)**. With a further increase of $\hat{t}$, the region between the two arrows is eventually occupied by the newly formed two pairs of cells, as seen from **Fig. 4(c)**. In this manner the initial three pairs evolve into two during the time interval indicated.

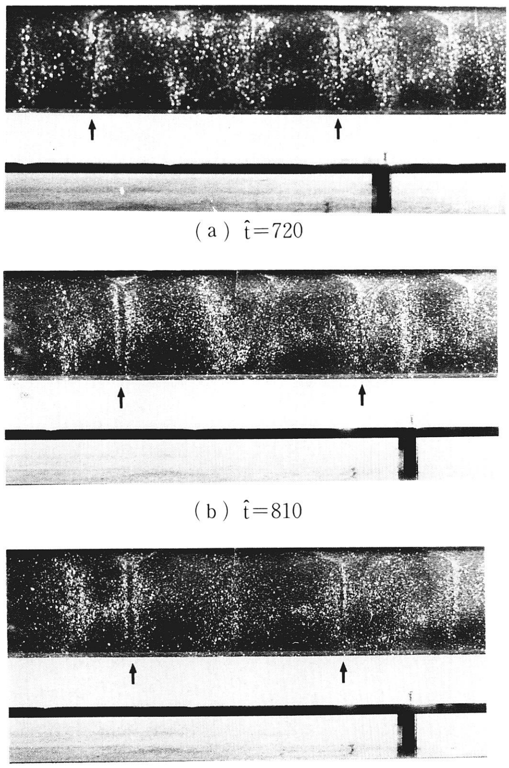

(a) $\hat{t}=720$

(b) $\hat{t}=810$

(c) $\hat{t}=1010$

Fig. 4 Merging of convective cells at Ra$=1.60\times10^5$, Pr$=5.80\times10^3$, and H$=0.06$ m

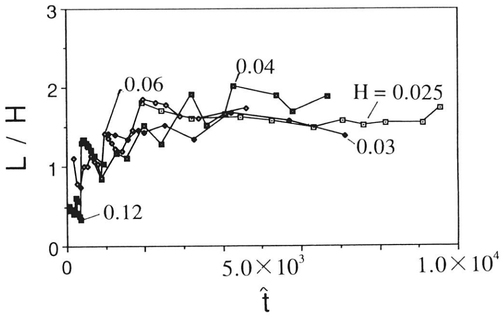

Fig. 5 $\hat{t}$-dependence of L/H at different values of H

The results of measurements of L/H is shown in **Fig. 5**, in which L/H is plotted against $\hat{t}$ at different values of H. Only the cell pattens apart from the both side walls were employed for measuring L. The values of L and their fluctuations increase with increasing H, as the freedom of fluid motion increases as the fluid layer becomes deep. **Figure 5** shows that L/H appear to settle at a constant value between 1.6 and 1.8 as the system evolves into a stationary state with increasing $\hat{t}$.

3. Numerical Analysis

3.1 Basic Equations and Numerical Schemes

The dimensionless vorticity and heat conduction equations governing 2D convective flows are

$$\frac{\partial \hat{\omega}}{\partial \hat{t}}+\frac{\partial \hat{\Psi}}{\partial \hat{y}}\frac{\partial \hat{\omega}}{\partial \hat{x}}-\frac{\partial \hat{\Psi}}{\partial \hat{x}}\frac{\partial \hat{T}}{\partial \hat{y}}=\nabla^2 \hat{\omega}+\frac{Ra}{Pr}\cdot\frac{\partial \hat{T}}{\partial \hat{x}}, \tag{4}$$

$$\nabla^2\hat{\Psi}=-\hat{\omega}, \tag{5}$$

and

$$\frac{\partial \hat{T}}{\partial \hat{t}}+\frac{\partial \hat{\Psi}}{\partial \hat{y}}\frac{\partial \hat{T}}{\partial \hat{x}}-\frac{\partial \hat{\Psi}}{\partial \hat{x}}\frac{\partial \hat{T}}{\partial \hat{y}}=\frac{1}{Pr}\cdot\nabla^2\hat{T}, \tag{6}$$

where $\hat{x}$, $\hat{y}$, $\hat{T}$, $\hat{\omega}$, and $\hat{\psi}$ are the non-dimensionalized horizontal and vertical coordinates, fluid temperature, vorticity, and streamfunction for the flows. These are intoduced as $\hat{x}=x/H$, $\hat{y}=y/H$, $\hat{T}=T/\Delta T$, $\hat{\omega}=\omega H^2/\nu$, and $\hat{\psi}=\psi/\nu$, where x, y, T, ω, and ψ are the corresponding dimensional parameters. Hereafter, however, the carets are suppressed for brevity.

In solving the equations, it is assumed that the fluid layer is heated from below and a constant temperature gradient is initially set up throughout the layer. The imposed initial and boundary conditions are as follows:

$$\begin{aligned}&\psi=0,\ \omega=0,\ T=1-y\ ;\ t=0\\&\psi=0,\ \omega=0,\ T=0\ ;\ y=1\\&\psi=0,\ \omega=\omega(I,1),\ T=1\ ;\ y=0\\&\psi=0,\ \omega=0,\ \partial T/\partial x=0\ ;\ x=0,\ b/H,\end{aligned} \tag{7}$$

where I indicates the horizontal mesh number and b is the horizontal length of a fluid layer used in calculation.

The basic equations (4), (5), and (6) discretized and numerically integrated to obtain convective cellular flow patterns, with the aid of the S. O. R. method. The dimensionless time step is taken as 1.0×10^{-3}, and the dimensionless spatial difference as 0.1 in the x and y directions ; in calculation an upwind numerical scheme is employed. The parameters Ra and Pr ranged $2.0\times10^{3}-2.5\times10^{4}$ and 0.7−70, respectively. As the boundary condition at y=0,

$$\omega_1=\frac{\Psi_3-8\Psi_2}{2\Delta y^2}$$

is imposed which is obtained by expanding ψ's and setting the velocity u=0 on the boundaries.

A set of random number disturbances is used to simulate an initial heating condition for the system. The disturbance amplitude ranges from -0.5 to 0.5, which are imposed on T at $y=0$ only for a single calculation time-step. The random numbers are generated by

$$Rn = (p \times Rn-1+c) \bmod M \quad ,$$

where $p=163$, $c=656329$, and $M=12518383$, with

$$RAND = R_n/M - 0.5 \quad ,$$

where RAND corresponds to the above mentioned amplitude. The output solutions are judged as stationay when the condition

$$\frac{\max \mid \omega_{i,j}^{k+1} - \omega_{i,j}^{k} \mid}{\max \mid \omega_{i,j}^{k+1} + \omega_{i,j}^{k} \mid} < 1.0 \times 10^{-4}$$

comes to be satisfied over the entire calculation region consisting of 10 (vertical) $\times$ 400 (horizontal) meshes.

3.2 Numerical Results

The results of numerical calculations are displayed as contour line maps of ψ and ω. Based on these results the numbers of cells formed in the fluid layer are read to compute L/H, which are tabulated in **Table 2** with cell n. stands for the number of cells.

Table 2 Numerical values of L/H

Pr Ra	0.7 cell n.	 L/H	7.0 cell n.	 L/H	50 cell n.	 L/H	70 cell n.	 L/H
2.00×10^{3}	39	2.1	39	2.1	32	2.5	26	3.1
2.50×10^{3}	40	2.0	40	2.0	40	2.0	36	2.2
3.50×10^{3}	40	2.0	40	2.0	44	1.8	40	2.0
5.00×10^{3}	50	1.6	50	1.6	50	1.6	50	1.6
7.50×10^{3}	50	1.6	50	1.6	50	1.6	50	1.6
1.00×10^{4}	50	1.6	48	1.7	50	1.6	50	1.6
1.25×10^{4}	52	1.5	48	1.7	50	1.6	50	1.6
1.50×10^{4}	52	1.5	44	1.8	50	1.6	50	1.6
2.00×10^{4}	50	1.6	38	2.1	50	1.6	50	1.6
2.50×10^{4}	50	1.6	38	2.1	50	1.6	49	1.6

The ψ-, ω-, and isothermal contour lines at $Ra=5.0\times10^{3}$ and $Pr=7.0$ are displayed respectively in **Figs. 6, 7**, and **8**; only the portions at $20<x<30$ are displayed here.

In **Fig. 6(a)**, the fluid layer is occupied by an irregular array of developing cells. This stage reflects the initially introduced random disturbances. As time advances with increasing $\hat{t}$ the irregular cells change into the regular ones. A stationary flow is shown in **Fig. 6(e)**, in which the regular cells occupy the entire fluid layer. A similar trend is also seen from **Fig. 7**, showing the ω distibutions. **Figure 8** shows that the isothermal lines are quite regular in a stationary flow.

The Ra-dependence of L/H at different values of Pr is displayed in **Fig. 9**. Its

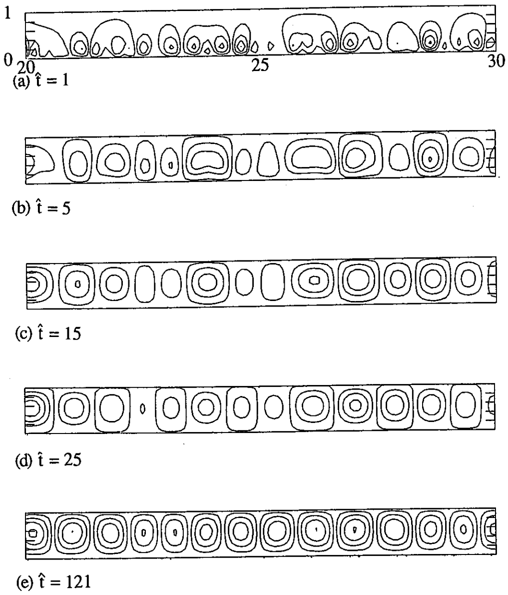

Fig. 6 Streamline contours at Ra=5.0×10^3 and Pr=7.0

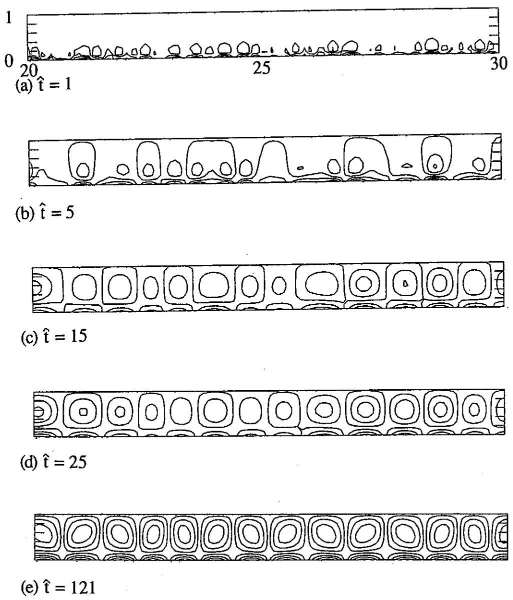

Fig. 7 Vorticity contour lines at Ra=5.0×10^3 and Pr=7.0

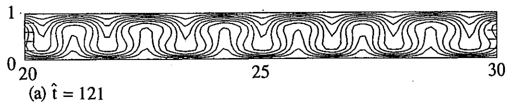

Fig. 8 Isothermal lines at Ra= 5.0×10^3, Pr=7.0 and t̂=121

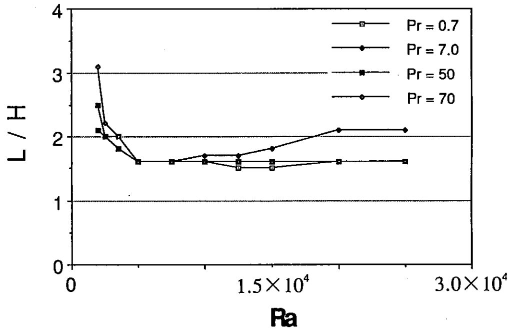

Fig. 9 Ra-dependence of L/H at different values of Pr

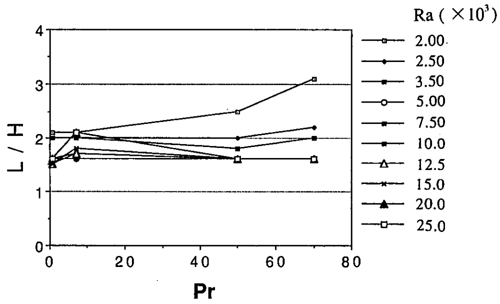

Fig. 10 Pr-dependence of L/H at different values of Ra

dependence on Pr at different values of Ra is displayed in **Fig. 10**. The Ra-dependence of L/H is conspicuous at smaller Ra (Ra < 5.00×10^3) and larger Pr. At Pr=70, L/H for small Ra is almost double that for large Ra. At large Ra > 5.00 × 10^3, L/H takes a constant value of about 1.6. The Pr-dependence of L/H is more conspicuous as Ra becomes smaller, and the L/H value is likely to increase with increasing Pr. The Ra- and Pr-dependence of L/H is summarized in **Fig. 11**, which indicates that the cells having large horizontal dimensions form at small Ra

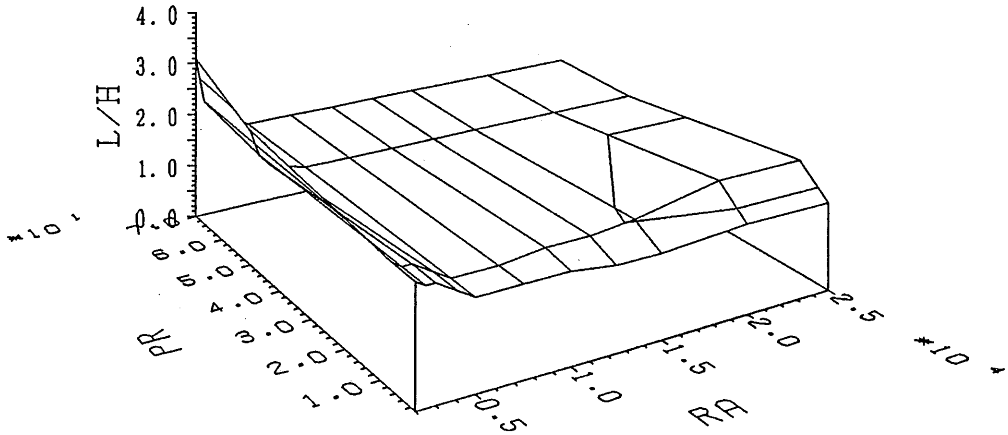

Fig. 11 Ra- and Pr-dependence of L/H for stationary convective cells

and large Pr.

It will be seen from **Fig. 9** that the Ra-dependence of L/H changes at $Ra=5.00\times10^3$. When $Ra<5.00\times10^3$, L/H takes a value between 1.6 and 3.1. When $Ra>5.00\times10^3$, L/H lies between 1.5 and 1.6 except for $Pr=7.0$. In other words, the Ra- and Pr-dependence of L/H is conspicuous when $Ra<5.00\times10^3$, and above this Ra there is no conspicuous Ra- and Pr-dependence. This means that the cells are stable when ΔT is small and both of κ and ν are large. Above $Ra=5.00\times10^3$ and at large Ra numbers, L/H takes a constant value in the range of 1.5~1.6, which agrees approximately with the experimental range of values between 1.6 and 1.8.

4. Conclusions

The procedures and results of the experiments and numerical analysis have been described concerning the 2D convective cellular flows formed in a horizontal long layer of fluid. The conclusions are summarized as follows.

1) The experimentally observed value of L/H for stationary cells is about 1.7 at $1.40\times10^4\leqq Ra\leqq1.20\times10^6$ and $4.80\times10^3\leqq Pr\leqq6.00\times10^3$.

2) The value of L/H based on the numerical calculation takes a value between 1.6 and 3.1 at $Ra<5.00\times10^3$. Above this Ra value, L/H is in between 1.5 and 1.6, which does not conspicuously depend on Ra and Pr. This value of L/H agree with the experimental value of 1.7, although the imposed boundary conditions and the range of Pr are not necessarily the same as the experimental ones.

Acknowledgements

The authers would like to thank Messrs. S. Yamashita, H. Fujimori, K. Sakai, H. Mizui, and Mrs. Y. Arizumi of the Geofluid Systems Dynamics Research Section for their help in the course of this work. The first author (S. K.) is also indebted to her classmates of the Department of Earth System Science & Technology for their encouragement. The work is partially supported by the Grant-In-Aid for Scientific Research from the Ministry of

Education, Science, and Culture, which is gratefully acknowledged.

References

1) C. Normand, Y. Pomeau and G. V. Manuel: Convective instability: A physicist's approach, Rev. Mod. Phys, **Vol. 49**, No. 3, (1977) 581-624.

2) J. S. Turner: Convection and mixing in the oceans and the Earth, Phys. Fluids **A3** (5), (1991) 1218-1232.

3) E. W. Bolton and F. H. Busse: Stability of convection rolls in a layer with stress-free boundaries, J. Fluid Mech. **150** (1985) 487-498.

4) M. Schnaubelt and F. H. Busse: On the stability of two-dimensional convection rolls in an infinite Prandtl number fluid with stress-free boundaies, Z. Angew. Math. Phys. **40** (1989) 153-162.

5) M. Kanda and M. Hino: Proceedings of Hydraulic Engineering, **Vol. 36** (1992) 501-506.